João Alves de Oliveira Neto
Instituto Tecnológico de Aeronáutica
São José dos Campos – Brazil
alves@ita.br

Edson Basso
Instituto de Aeronáutica e Espaço
São José dos Campos – Brazil
edsonbassoeb@iae.cta.br

João Luiz F. Azevedo*
Instituto de Aeronáutica e Espaço
São José dos Campos – Brazil
joaoluiz.azevedo@gmail.com

*author for correspondence

Aerodynamic study of sounding rocket flows using Chimera and patched multiblock meshes

Abstract: *Aerodynamic flow simulations over a typical sounding rocket are presented in this paper. The work is inserted in the effort of developing computational tools necessary to simulate aerodynamic flows over configurations of interest for Instituto de Aeronáutica e Espaço of Departamento de Ciência e Tecnologia Aeroespacial. Sounding rocket configurations usually require fairly large fins and, quite frequently, have more than one set of fins. In order to be able to handle such configurations, the present paper presents a novel methodology which combines both Chimera and patched multiblock grids in the discretization of the computational domain. The flows of interest are modeled using the 3-D Euler equations and the work describes the details of discretization procedure, which uses a finite difference approach for structure, body-conforming, multiblock grids. The method is used to calculate the aerodynamics of a sounding rocket vehicle. The results indicate that the present approach can be a powerful aerodynamic analysis and design tool.*
Keywords: *Chimera grids, Patched multiblock grids, Sounding rockets.*

INTRODUCTION

In the present work, the results obtained for the simulation of aerodynamic flows concerning a typical sounding rocket, SONDA-III, are presented. This work is inserted into the effort of development of computational tools necessary to simulate aerodynamic flows over aerospace geometries, especially those related to the Brazilian Satellite Launcher (VLS, acronym in Portuguese). Details of the work developed so far, as well as results that illustrate the advancements that have been accomplished up to now in this long term research effort, can be seen, among other references, in Azevedo, Menezes and Fico Jr. (1996), Azevedo, Strauss and Ferrari (1997), Strauss and Azevedo (1999), Bigarella (2007) and Bigarella and Azevedo (2007). The SONDA-III presents a quite complex geometric configuration with four front fins and four back fins around a central core. The fins are arranged symmetrically around the central body. An illustrative outline of this configuration is presented in Fig. 1, including a closer view of the frontal fin region.

The research group has a fair amount of experience with Chimera and patched multiblock flows simulations for

launch vehicle aerodynamics. The present application represents, however, the first time that the group used the two techniques in the same code. This is also the first time that the group simulates a vehicle with fins. The fundamental objective of the present effort is, therefore, to demonstrate that the use of the two techniques combined will enable the generation of better quality grids for the problems at hand. Hence, the major contribution of the present work rests upon the creation of the capability of simulating the flow over launch vehicles with fins, using a combined patched-Chimera grid approach.

The governing equations are assumed written in conservative form and they are discretized in a finite diference context. Spatial discretization uses second-order accurate, central diference operators. The time march method is based on a five-stage, Runge-Kutta algorithm described in Jameson, Schmidt and Turkel (1981), which also has second-order accuracy in time. The artificial dissipation terms added are based on the nonisotropic artificial dissipation model described in Turkel and Vatsa (1994). In the present case, Chimera and patched grid techniques are used to simulate ows over the complete SONDA-III sounding rocket. These techniques together provide the capability to use structured meshes for the discretization of the calculation domain over truly complex configurations. The paper
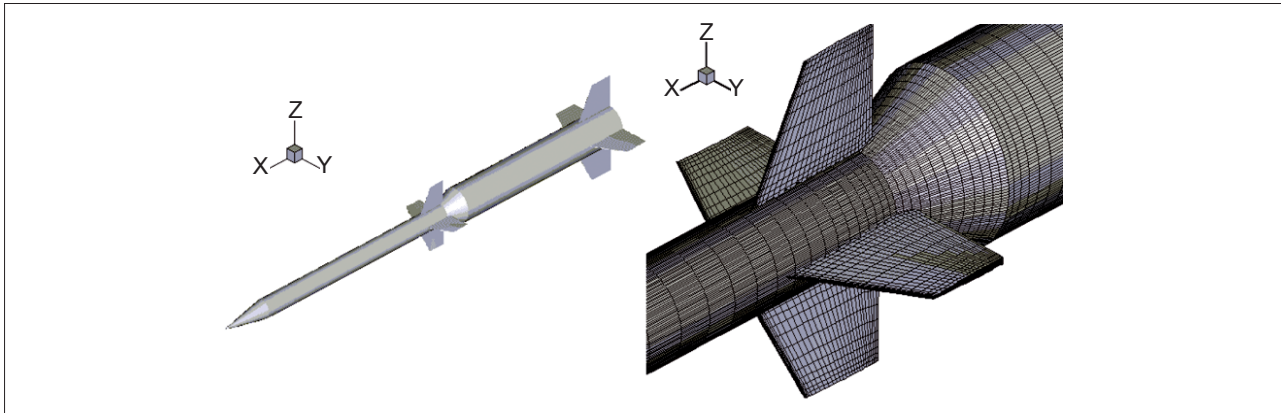
Figure 1: Perspective view of the SONDA-III (left) and detail of the front fin region (right).

will briefly describe the theoretical formulation used with a discussion of the numerical implementation aspects. Details of the current implementation of Chimera and patched grid techniques are also presented, with the boundary conditions adopted. Results with applications to SONDA-III are described and some concluding remarks are presented.

THEORETICAL FORMULATION

In the present work, it is assumed that the flows of interest can be represented by the Euler equations in three spatial dimensions. These equations can be written in conservative law form, in a curvilinear coordinate system:

$$\frac{\partial \overline{Q}}{\partial \tau} + \frac{\partial \overline{E}}{\partial \xi} + \frac{\partial \overline{F}}{\partial \eta} + \frac{\partial \overline{G}}{\partial \zeta} = 0 \qquad (1)$$

where $\bar{E}$, $\bar{F}$ and $\bar{G}$ are the inviscid flux vectors, which can be seen in more detail in Vieira *et al.* (1998), and Q is the vector of conserved variables, defined as:

$$\overline{Q} = J^{-1}[\rho \; \rho \upsilon \; \rho \upsilon \; \rho \omega \; e]^{\mathrm{T}} \qquad (2)$$

where ρ is the density, u, v and w are the Cartesian velocity components, e is the total energy per unit volume and J is the Jacobian of the transformation, represented as (Eq. 3):

$$J = (x_\xi y_\eta z_\zeta + x_\eta y_\zeta z_\xi + x_\zeta y_\xi z_\eta - x_\xi y_\zeta z_\eta - x_\eta y_\xi z_\zeta - x_\zeta y_\eta z_\xi)^{-1} \qquad (3)$$

The pressure can be obtained from the equation of state for a perfect gas:

$$p = (\gamma - 1)\left[e - \frac{1}{2}\rho(u^2 + v^2 + w^2)\right] \qquad (4)$$

A suitable nondimensionalization of the governing equations has been assumed in order to write Eq. 1. In particular, the values of flow properties are made dimensionless with respect to freestream quantities, as described in Pulliam and Steger (1980). The governing equations were discretized in a finite diference context in structured hexahedral meshes which would conform to the bodies in the computational domain. Since a central difference spatial discretization method is used, artificial dissipation terms must be added to the formulation in order to control nonlinear instabilities. The artificial dissipation terms used here are based in the work of Turkel and Vatsa (1994). This model is nonlinear and nonisotropic, with the scaling of the artificial dissipation operator in each coordinate direction weighted by its own spectral radius of the corresponding flux Jacobian matrix. In the present implementation, the residue operator is defined as:

$$RHS^n = -\Delta t(\delta_\xi E^n + \delta_\eta F^n + \delta_\zeta G^n) \qquad (5)$$

where δ_ξ the δ_ζ and δ_η terms represent mid-point central diference operators in the ξ, ζ and η directions, respectively. The numerical flux vectors and artificial dissipation operators are defined as:

$$E_{i\pm\frac{1}{2},j,k} = \frac{1}{2}(E_{i,j,k} + E_{i+1,j,k)} - d_{i\pm\frac{1}{2},j,k,}$$

$$F_{i,j\pm\frac{1}{2},k} = \frac{1}{2}(F_{i,jk} + F_{i,j+1,k}) - d_{i,j\pm\frac{1}{2},k,}$$

$$G_{i,j,k\pm\frac{1}{2}} = \frac{1}{2}(G_{i,j,k} + E_{i,j,k+1}) - d_{i,j,k\pm\frac{1}{2}}. \qquad (6)$$

The artificial dissipation operators are defined precisely as described in Turkel and Vatsa (1994). Since steady state solutions are the major interest in the present study, a variable time step convergence acceleration procedure has been implemented. The time march is performed based on

a five-stage, second-order accurate, hybrid Runge-Kutta time-stepping scheme, which can be written as:

$$Q_i^{(0)} = Q_i^n,$$
$$Q_i^{(1)} = Q_i^{(0)} - \alpha_1 RHS^{(0)},$$
$$Q_i^{(2)} = Q_i^{(0)} - \alpha_2 RHS^{(1)},$$
$$Q_i^{(3)} = Q_i^{(0)} - \alpha_3 RHS^{(2)},$$
$$Q_i^{(4)} = Q_i^{(0)} - \alpha_4 RHS^{(3)},$$
$$Q_i^{(5)} = Q_i^{(0)} - \alpha_5 RHS^{(4)},$$
$$Q_i^{n+1} = Q_i^{(5)}, \tag{7}$$

where $\alpha_1 = 1/4$, $\alpha_2 = 1/6$, $\alpha_3 = 3/8$, $\alpha_4 = 1/2$ and $\alpha_5 = 1$. The time step is defined as (Eq. 8):

$$\Delta t_{i,j,k} = \frac{CFL}{c_{i,j,k}} \tag{8}$$

The CFL acronym stands for the Courant-Friedrichs-Lewy number, and the characteristic speed $c_{i,j,k}$ is defined as:

$$c_{i,j,k} = \max\left(|U| + a\sqrt{\xi_x^2 + \xi_y^2 + \xi_z^2}, |V| + a\sqrt{n_x^2 + n_y^2 + n_z^2}, |W| + \right.$$
$$\left. a\sqrt{\zeta_x^2 + \zeta_y^2 + \zeta_z^2} \right) \tag{9}$$

where a is the speed of sound and U, V and W are the contravariant velocity components. It should be emphasized that only the convective operator inside RHS term indicated in Eq. 8 is actually evaluated at every time step. The artificial dissipation term is only evaluated in the first and second stages of the time march procedure. It can be shown that this provides enough damping to maintain nonlinear stability, as defined in Jameson, Schmidt and Turkel (1981), whereas it yields a more efficient numerical scheme.

COMPUTATIONAL GRID TOPOLOGY

SONDA-III rocket possesses a central body where four frontal fins and four back fins are mounted. In order to save computational resources, 1/8 of the complete configuration in the azimutal direction was simulated. This simplification is valid in the present work because only simulations with zero attack-of-angle are considered. In this way, taking advantage of the symmetry of the problem, the configuration is reduced to 1/8 of the central body in the azimutal direction, 1/2 of the frontal fin and 1/2 of the back fin. In total, 13 meshes with relatively simple geometry are used to model the rocket and the fins. These meshes are distributed in the following way:

- seven meshes for the front fin, denominated m_1, m_2, m_3, m_4, m_6 and m_7;

- three meshes for the back fin, denominated m_9, m_{10} and m_{11};

- one mesh for central body, denominated m_{13}, as seen in Fig. 2;

- one (background) mesh for front fin, denominated m_8, as seen in Fig. 2;

- one (background) mesh for back fin, denominated m_{12}, as seen in Fig. 2.

The computational meshes used in the present work are all generated by algebraic methods within each block. In particular, the multisurface algebraic grid generation technique described by Fletcher (1991) has been implemented in a fairly general code for the present configurations. The code allows grid clustering at various regions and a fair amount of control on the grid point distribution along the normal direction. Both hyperbolic tangent and exponential grid stretching functions are used to obtain the desired clustering and coarsening of the grid over the body. The meshes generated by that method are 2-D. The mesh that discretizes the central body is rotated around the longitudinal axis, obtaining a 3-D mesh. Initially, for the fins, 2-D meshes are generated for the root and top sections. These meshes can be seen in detail in Fig. 3. The root surface is deformed through
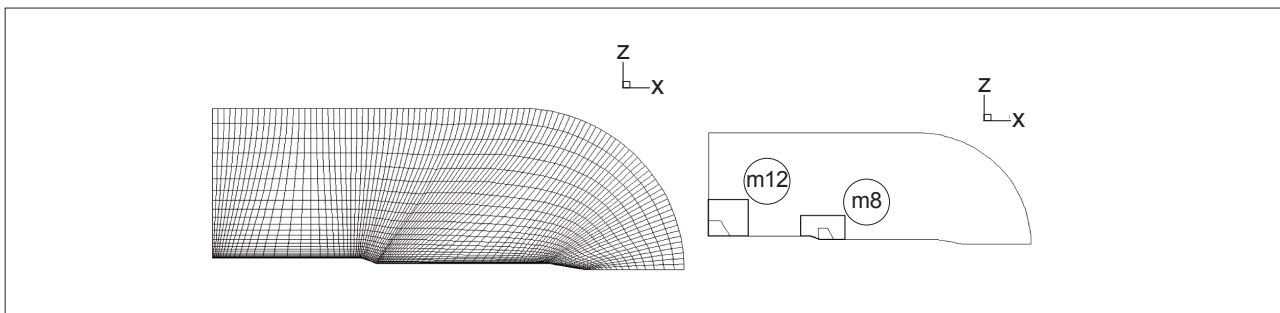

Figure 2: Central body mesh (left) and the m_8 and m_{12} background meshes (right).
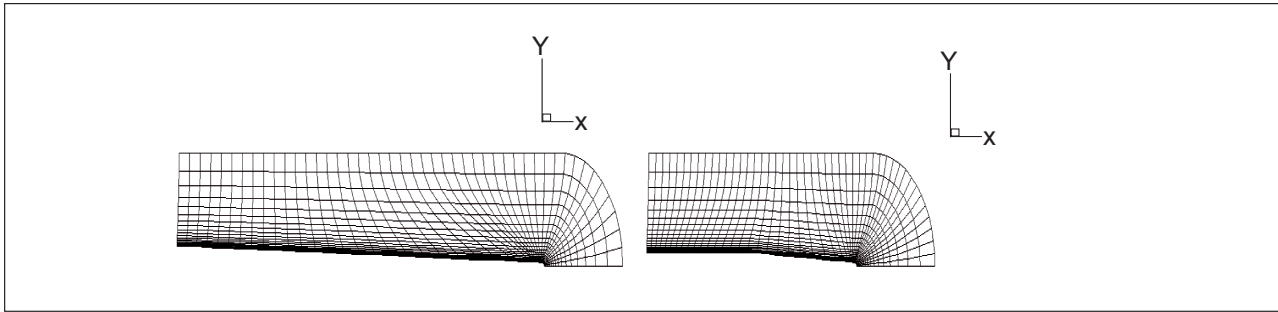
Figure 3: Two-dimensional surface on the root (left) and on the top (right) of the front fin generated by an algebraic method.

a coordinate transformation to conform to cylindrical and conical sections of the central body. Finally, intermediate surfaces are obtained through an interpolation from the top and bottom surfaces previously calculated, as shown in Fig. 4.
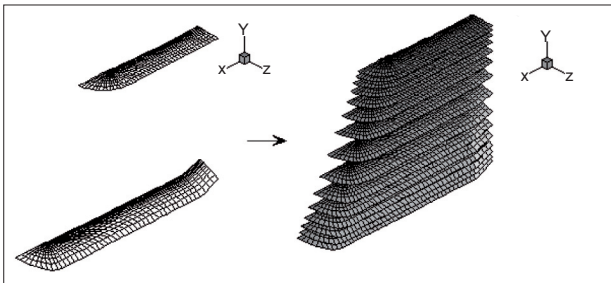

Figure 4: Intermediate surfaces obtained by interpolation of the tip and root surfaces of the front fin.

Previous work on tridimensional configuration of launch vehicles, using the VLS configuration, as can be seen in Basso, Antunes and Azevedo (2003), used only Chimera grids to discretize the computational domain. However, during the initial phase of planning of the meshes for SONDA-III, the research group noticed that, due to the geometric characteristics of the new problem, using only Chimera meshes would not be viable.

The adopted solution was to use Chimera in conjunction with patched grids, since this procedure allowed the generation of meshes in a much simpler way, in comparison with other proposals that just used one technique or another. The Chimera subroutines of the original solver for the VLS were adapted, and additional subroutines were implemented for the use of patched grids. Routines for the control of the flow of information among the meshes were also implemented, and all the particularities of the original code (Antunes, 2000; Basso, Antunes and Azevedo 2003) for the configuration of the VLS were eliminated. With that, the research group developed a somewhat general code that can work with Chimera and patched grids, in complex configurations. The number of meshes that the code can manage is just limited by the amount of memory of the machine.

Basically, the m_1 to m_7 meshes, that involve the front fin, exchange information amongst themselves using the patched mesh technique. These seven meshes exchange information, through of the Chimera interfaces with the m_8 mesh (*background* mesh), and finally, the m_8 mesh exchanges information with the central body mesh, m_{13}. For the back fins, the process is similar. The *background* meshes, m_8 and m_{12}, have the function of serving as transition between the fin meshes, that possess a large number of points, and the central body mesh, that possesses few points. Besides, the background meshes hide the complexity of the configuration, since the central body mesh does not see the fin meshes. If the background meshes were not used, the central body mesh would have many more points in order to communicate in an efficient way with the fin meshes. The flow of information among the meshes can be seen in Fig. 5.
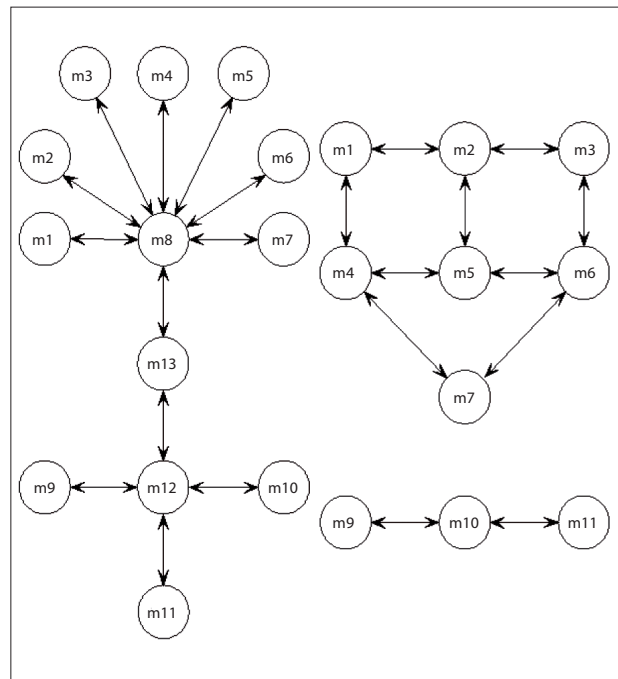

Figure 5: Information flow of the Chimera meshes (left) and the patched meshes (right).

BOUNDARY CONDITIONS

For the configurations of interest here, the types of boundary conditions that should be considered include upstream (entrance), solid-wall, far-field, symmetry, upstream centerline and downstream (exit) conditions. The upstream centerline of the rocket grid is a singularity of the coordinate transformation and, hence, an adequate treatment for this boundary must be provided. The approach consists in extrapolating the property values from the adjacent longitudinal plane and averaging the extrapolated values in the azimuthal direction in order to define the updated properties at the upstream centerline.

The vast majority of the previous experience of the research group in the use of Chimera or patched multiblock grids considered the VLS configuration (Basso, Antunes and Azevedo, 2003; Bigarella, 2007), without including afterbody or plume effects. For such a configuration, the number of grid blocks required is rather small. Therefore, it is possible to have the boundary conditions hard-coded for each specific case. However, in the present case, the procedure of writing 13 separate subroutines to work with the 13 meshes would be extremely difficult and prone to mistakes. Furthermore, the objective should always be to try to come up with a code as general as possible and, certainly, it should not depend on the particularities of the configuration under consideration. Again, the approach is to eliminate the particularities of the original code and to create a more powerful subroutine that could work with the diversity of boundary conditions that the meshes of SONDA-III present.

The blocks of the mesh are considered as hexahedra in computational space and each one of the six faces is numbered as indicated in Fig. 6. The code, that represents a certain boundary condition, is associated to each face. With this method, the solver implements 78 boundary conditions in a simple format for the user. The boundary conditions and the number of points of each block of the mesh can be observed in Table 1. In case one wants to change some boundary conditions, it is sufficient to alter the values of a table, without the need to modify any code line.
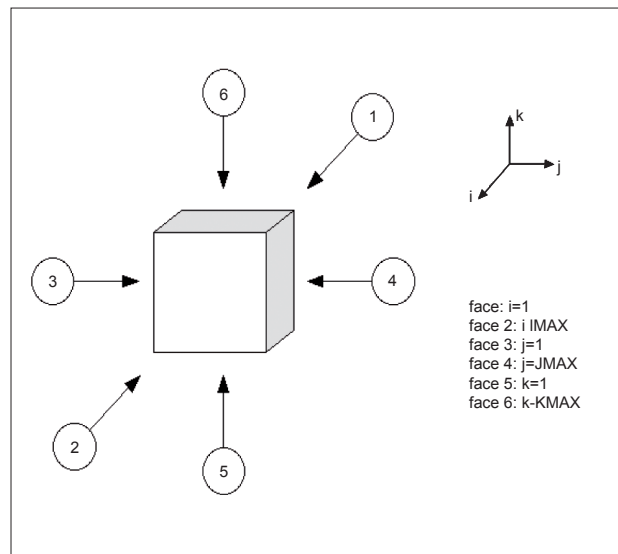

Figure 6: Definition of the meshes faces for the boundary conditions.

Table 1: Boundary conditions imposed in the mesh faces.

Mesh	Face 1	Face 2	Face 3	Face 4	Face 5	Face 6	Points
m_1	patched	symmetry	wall	Chimera	patched	wall	65,340
m_2	patched	symmetry	patched	Chimera	patched	Chimera	53,460
m_3	patched	symmetry	patched	symmetry	wall	Chimera	53,460
m_4	patched	Chimera	patched	Chimera	patched	wall	26,136
m_5	patched	Chimera	patched	Chimera	patched	Chimera	21,384
m_6	patched	Chimera	patched	symmetry	patched	Chimera	21,384
m_7	wall	Chimera	patched	symmetry	patched	wall	26,136
m_8	Chimera	Chimera	symmetry	symmetry	wall	Chimera	137,940
m_9	exit	symmetry	wall	Chimera	patched	wall	65,340
m_{10}	exit	symmetry	patched	Chimera	patched	Chimera	53,460
m_{11}	exit	symmetry	patched	symmetry	wall	Chimera	53,460
m_{12}	exit	Chimera	symmetry	Chimera	symmetry	Chimera	117,612
m_{13}	exit	centerline	wall	freestream	symmetry	symmetry	192,375

TREATMENT OF PATCHED GRID INTERFACES

In the present work, a patched grid block always shares a common face of points with other patched grid block, as indicated in Fig. 7. In order to illustrate this procedure, it is assumed that there are two meshes, denominated A and B, as presented in Fig. 7. Those meshes should be expanded, in order to allow the implementation of a code with the capability of transferring information through the common faces. It is desirable to maintain the order of the artificial dissipation operators at all points. Therefore, taking into account that the artificial dissipation operators use five points, a possible solution is to expand the meshes such that there is an area of five rows of points in common, as indicated in the right side of Fig. 7.

It can be observed that two rows of points were added to each mesh, which caused the displacement of the first column of points. The following steps are executed:

1. Initially, the properties of all interior points located in the expanded A mesh are calculated, advancing one step in time;

2. The points located in the first column of the B mesh receive the values of the properties of the points from the fifth column of the A mesh;

3. The points located in the second column of the B mesh receive the values of the properties of the points from the fourth column of the A mesh;

4. All the interior points of the B mesh are calculated, advancing one step in time for this mesh;

5. The values of the points located in the fifth column of the B mesh are transferred for the first column of the A mesh, and values of the fourth column of

the B mesh are transferred for the second column of the A mesh;

6. The interior points of the A mesh are calculated again and the process repeats.

The third column of the two meshes is left "free" and its value is determined by the calculation of the interior points, without any imposition of values for the properties, as it happened with the first and the second columns. Attempts of imposing any value for the properties in the third column − as, for example, an average between the two meshes − resulted in a significant decrease of the convergence rate. In 3-D, instead of lines or columns, the meshes have planes in common. In the present paper, the meshes are built with a single face in common, and an additional code takes care of reading a connection matrix to decide which faces of each mesh should be expanded. More details on this procedure can be found in Papa and Azevedo (2003).

THE CHIMERA HOLECUTTING PROCESS

The Chimera grid possesses a superposition area but, unlike the patched grid, there is no need for the points to coincide. Again, this area is responsible for the exchange of information among the meshes. However, as not all of the points are necessary for the communication among the meshes, one can logically eliminate some points. Actually, all of the points continue to exist in the computer memory. The user creates an auxiliary matrix that associates to each point of the mesh an on-value or an off-value. The points are eliminated by two reasons. The first one concerns the fact that points of a certain mesh may be located inside an area without physical meaning of another mesh as, for example, inside a body of some other component of the configuration. An example of such situation could be found in the points of the m_8 mesh that are located inside the front fin. The left side of Fig. 8 exhibits the m_8 mesh
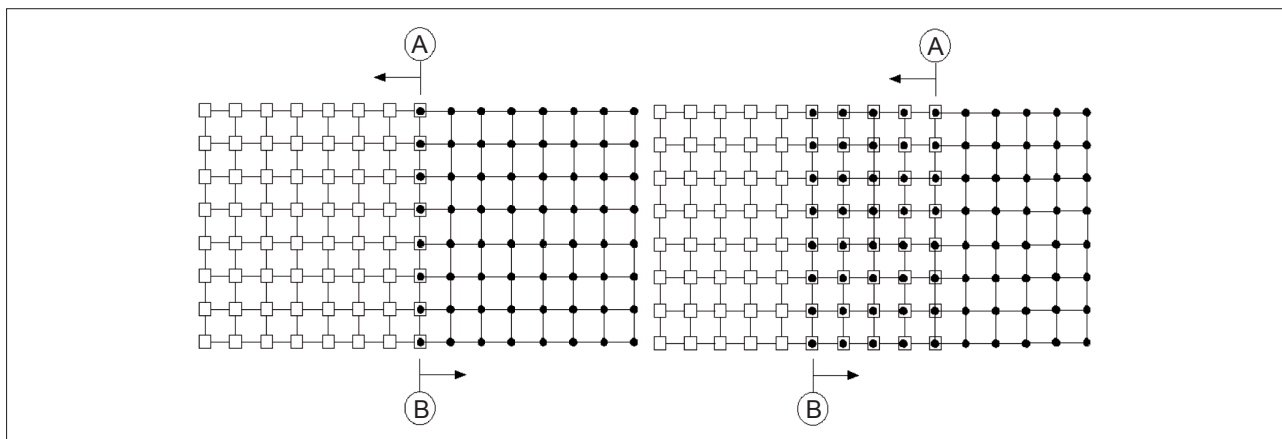

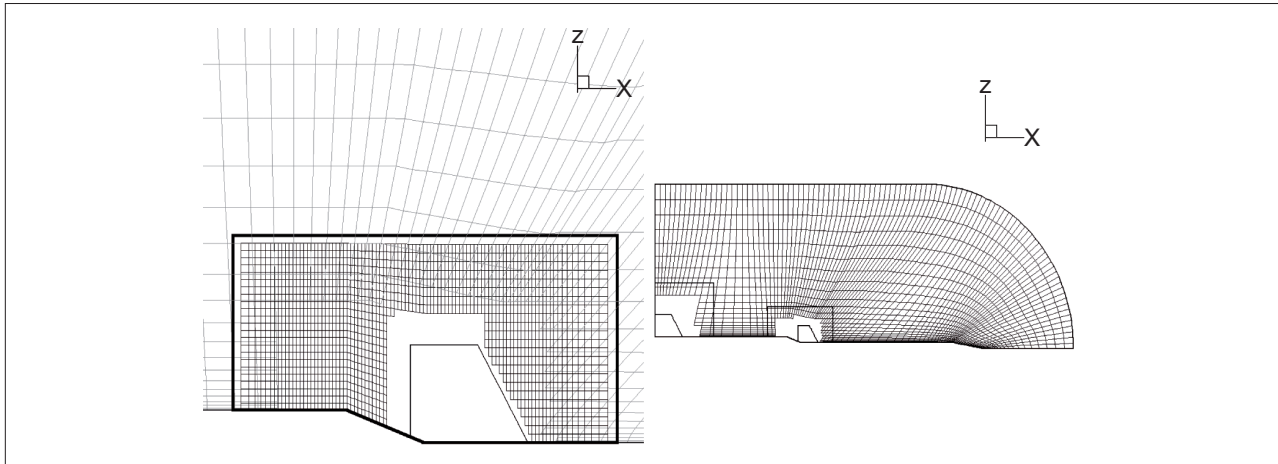Figure 7: A and B meshes before (left) and after (right) the expansion process.

Figure 8:   Detail of the m_8 background mesh (left) and m_{13} central body mesh (right) after the holecutting process.

with the points eliminated and the outline of the fin. In practice, a virtual volume larger than the solid volume is created, and all points of the mesh that are inside the virtual volume are eliminated. The creation of the virtual volume allows for the control of the number of points to be eliminated.

The second reason to eliminate points is to reduce the sobreposition area. An example can be found in the central body mesh, m_{13}, that contains the two background meshes, m_8 and m_{12}. A virtual volume completely contained in a background mesh is created and all points of the mesh, that are inside this volume, are eliminated. The right hand side in Fig. 8 displays the result of this process.

After the holecutting process, described in Antunes, Basso and Azevedo (2000), the next step consists in identifying the Chimera boundary points. These points are those which were not eliminated by the previous process, but they have at least one neighbor that was eliminated. The Chimera boundary points are not calculated in the same way as the other interior points. They have the values of their properties interpolated. Each Chimera boundary point is located inside of an hexahedron whose vertices are formed by points of the other Chimera grid. As described in Antunes (2000), the distances between a Chimera boundary point of the first mesh and each of the eight vertices of the second mesh are calculated, respectively. It should be emphasized that there is no attempt to satisfy conservation in the present interpolation process. Since shocks may be crossing the interface, it would be interesting to have the enforcement of some conservation statement at grid interfaces. However, this was not implemented in the present case due to the high computational costs associated with such implementation, especially in the 3-D case, and because the present effort should be seen as an evolutionary step towards a more complete simulation capability.

Furthermore, the use of a conservative interpolation process would certainly increase the requirements of code memory, which the authors would like to avoid at this time. An interpolation method at the interfaces among Chimera meshes that satisfies conservation was developed by Wang, Buning and Benek (1995). A detailed discussion of the procedure can be found in Wang and Yang (1994). Current work in this issue is also going on in the laboratory where the present work was developed (Pio *et al.*, 2010), but, as stated, this is beyond the scope of the present paper.

RESULTS AND DISCUSSION

The results presented refer to simulations of the flow over SONDA-III rocket during its first stage flight. Preliminary results for this configuration have been presented in Papa and Azevedo (2003). In the cited reference, however, the total number of grid points was of the order of 275,000, which did not allow for a more detailed visualization of some critical regions of the flow about the fins. The present work has performed similar simulations, however considering a much finer mesh, with approximately 900,000 grid points. Such a level of grid refinement allows for a considerably better visualization of flow details about the configuration. The specific results included here consider only the case with freestream Mach number $M_\infty = 2.0$ and zero angle-of-attack, which is representative of the simulations performed so far for the configuration.

Moreover, as the flight time in the lower atmosphere for these rockets is very short and the vehicle is at supersonic speeds during most of this flight, it seems appropriate to select a supersonic flight condition for the present discussion. As previously mentioned, the major interest in this work concerns the evaluation of the joint use of Chimera and patched grid techniques as

a tool for flow analysis over geometries of interest for Instituto de Aeronáutica e Espaço. Within the supersonic speed regime, several interesting aspects of Chimera and patched grid techniques can be analyzed, such as the communication of information across internal boundaries among blocks with discontinuities in the flow properties.

Figure 9 exhibits the residue history for all the meshes. The CFL number used is 0.9 and approximately 9,000 iterations are necessary in order to reach convergence. In Fig. 9, one can observe that the mesh with the slowest convergence rate is the one that contains the recirculation zone, i.e., the m_6 mesh. Mach number contours over the vehicle body, in regions around the front and back fins, can be observed in Figs. 10

and 11. These figures show in detail the region of interaction between the front and back fins and the conical region of the central body. One can observe that the thickness of the shock in the leading edge of the front fin increases when it approaches the plane of symmetry. Pressure contours for the sounding rocket and its front and back fins can be observed in Figs. 12 and 13. In these figures, one can observe the formation of shock waves in the leading edges of the fins, as well as the expansion regions in the trailing edges. In the conical region, there is an increase in pressure due to a shock wave that cannot be observed in these visualizations. It can also be observed that, after the conical region, the pressure decreases due to the expansion region in the intersection between the conical and cylindrical body regions.
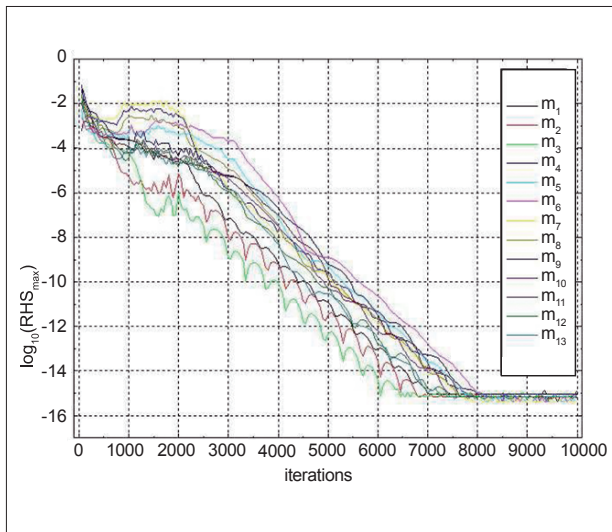

Figure 9:   Residue history for all the meshes used in the simulation ($M_\infty = 2.0$ and CFL = 0.9).
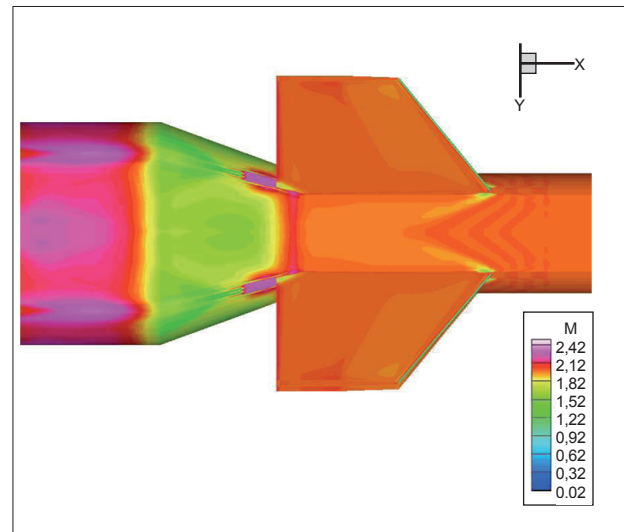

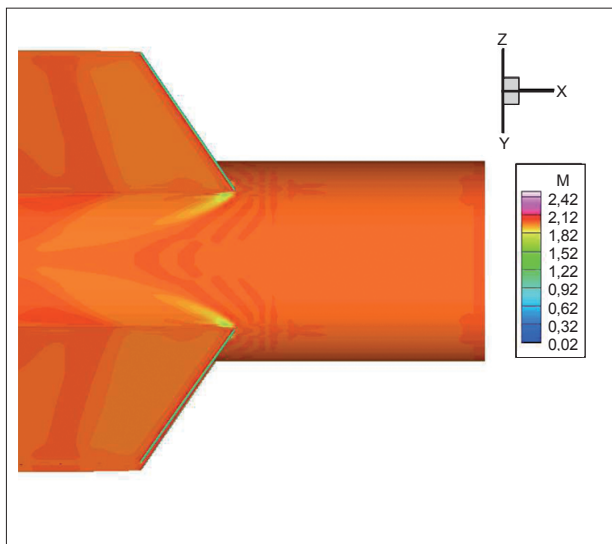Figure 11: Mach number contours for the front fin region.

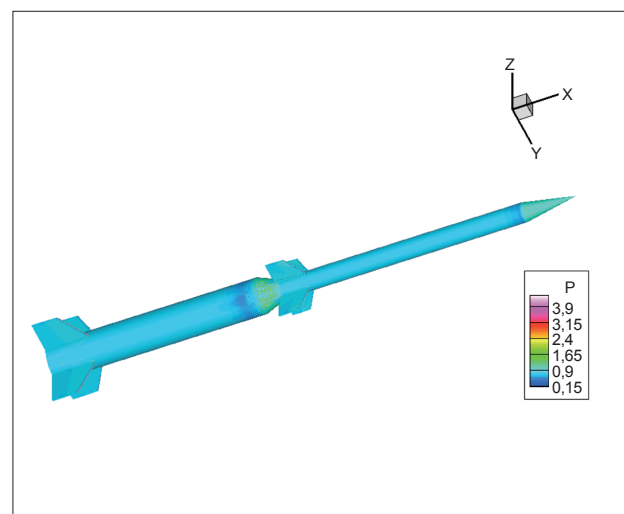Figure 10: Mach number contours for the back fin region.

Figure 12: Dimensionless pressure contours on the surface of the sounding rocket.
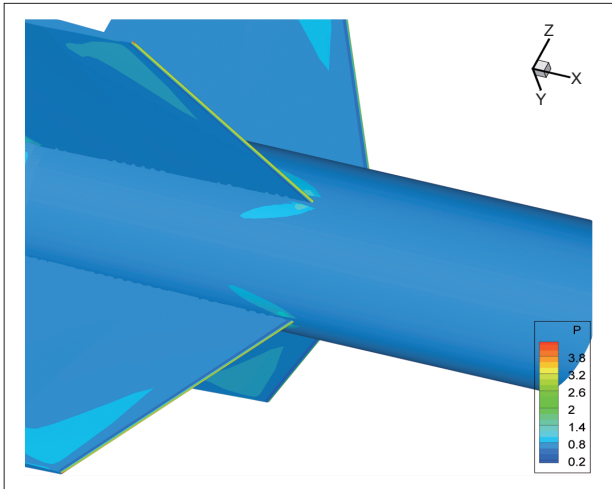
Figure 13: Dimensionless pressure contours on the front fin region.

It is important to emphasize that the Missile Datcom (Blake, 1998) approach is typically used for stability and control purposes. Furthermore, it is also important to emphasize that the calculations with the Missile Datcom approach were performed by the present authors themselves. From a physical perspective, one can observe that, essentially, at supersonic freestream conditions, there is an oblique shock impinging on the fins downstream of the cylinder intersection. A sudden increase in the pressure coefficient distribution is observed at $x/c = 9$, for the computational solution. The increase in pressure coefficient (Cp) is due to the oblique shock wave created by the compression corner along the central body. Finally, the reader should observe that the authors did not have access to experimental aerodynamic results for the present configuration. Therefore, the validation here discussed is performed using Missile Datcom data.

CONCLUDING REMARKS

The paper has presented results for 3-D Euler simulations of the flow over the SONDA-III vehicle, a typical sounding rocket. A structured multiblock code has been implemented, using Chimera and patched multiblock grid approaches for handling the geometric complexity of the configuration. All codes used were developed by the research group and represent a powerful aerodynamic analysis and design
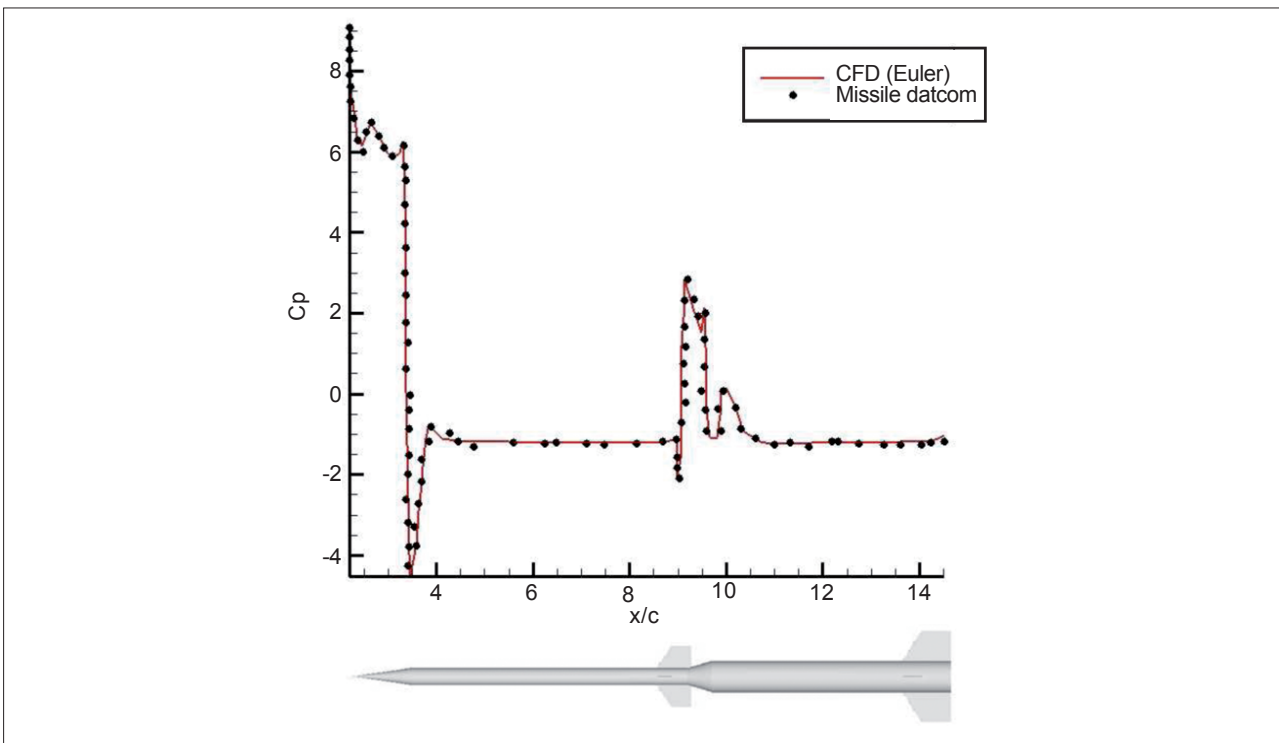
Figure 14 shows a quantitative comparison of the results obtained in the present computations. The numerical pressure coefficient distribution over a longitudinal line along the vehicle, which is located half way between two fins, is shown to be in very good agreement with results obtained with the Missile Datcom approach (Blake, 1998). Such program is a widely used semi-empirical data sheet component build-up method for estimating the aerodynamic characteristics of missiles and other rocket-like bodies.

Figure 14: Cp distributions over the SONDA-III at $M_\infty = 2.0$ and zero angle-of-attack.

tool. The present methodology, using a combination of Chimera and patched grid approaches, seems to be quite powerful to work on similar problems, even with the presence of several fins. The main advantages observed in the present approach are:

1. Flexibility: the joint use of Chimera and patched grids, in the same simulation, allows the generation of meshes in a much easier and quicker fashion than other competing approaches;

2. Modularity: the use of background meshes, hiding the complexity of the meshes that involve the fins, also seems to be a very interesting approach for these rocket-like configurations. With such an approach, small grid modifications, or even small configuration modification, are quite simple to be accommodated in the sense that one does not need to regenerate all the meshes or, even, to reschedule the flow of information;

3. Point concentration: the use of multiblock meshes allows the refinement of localized regions in a way very similar to unstructured meshes, hence providing the needed flexibility to discretize complex configurations.

Finally, the power of this combined Chimera and patched grid simulation capability becomes evident when one considers that it was possible to simulate the flow over a complete sounding rocket and, at the same time, to capture details of phenomena occurring along the trailing edge of the frontal fins. This indicates that the methodology presented allowed grid refinement characteristics similar to those found in unstructured meshes, without the inconvenience of indirect addressing, as described in Long, Khan and Sharp (1991).

ACKNOWLEDGEMENTS

REFERENCES

Antunes, A.P., 2000, "Simulation of aerodynamic flows using overset multiblock grids," M.S. Thesis, Instituto Tecnológico de Aeronáutica, São José dos Campos, SP, Brazil (in Portuguese, original title is "Simulação de Escoamentos Aerodinâmicos Utilizando Malhas de Blocos Múltiplos Sobrepostos").

Antunes, A.P., Basso, E., and Azevedo, J.L.F., 2000, "Holecut: a program for the generation of Chimera grids," Instituto de Aeronáutica e Espaço, CTA/IAE/ASE-N, São José dos Campos, SP, Brazil (in Portuguese, original title is "Holecut: Um Programa de Geração de Malhas Chimera").

Azevedo, J.L.F., Menezes, J.C.L., and Fico Jr., N.G.C.R., 1996, "Accurate turbulent calculations of transonic launch vehicles flows," Proceedings of the 14th AIAA Applied Aerodynamics Conference, AIAA Paper No. 96-2484-CP, Vol. 3, New Orleans, LA, USA, pp. 841-851.

Azevedo, J.L.F., Strauss, D., and Ferrari, M.A.S., 1997, "Viscous multiblock simulations of axisymmetric launch vehicle flows," Proceedings of the 15th AIAA Applied Aerodynamics Conference, AIAA Paper No. 97-2300-CP, Vol. 2, Atlanta, GA, USA, pp. 664-674.

Basso, E., Antunes, A.P., and Azevedo, J.L.F., 2003, "Chimera simulations of supersonic flows over a complex satellite launcher configuration," Journal of Spacecraft and Rockets, Vol. 40, No. 3, pp. 345-355.

Bigarella, E.D.V., 2007, "Advanced turbulence modelling for complex aerospace applications," Ph.D. Thesis, Instituto Tecnológico de Aeronáutica, São José dos Campos, SP, Brazil.

Bigarella, E.D.V., Azevedo, J.L.F., 2007, "Advanced eddy-viscosity and Reynolds-stress turbulence model simulations of aerospace applications," AIAA Journal, Vol. 45, No. 10, pp. 2369-2390.

Blake, W.B., 1998, "Missile Datcom – User's Manual," Wright-Patterson AFB, Ohio, USA.

Fletcher, C.A.J., 1991, "Computational techniques for fluid dynamics," Vol. 2, Spring-Verlag, NewYork, USA.

Jameson, A., Schmidt, W., and Turkel, E., 1981, "Numerical solutions of the Euler equations by finite volume methods using Runge-Kutta time-stepping schemes," Proceedings of the 14th Fluid and Plasma Dynamic Conference, AIAA Paper No. 81-1259, Palo Alto, CA, USA.

Long, L.N., Khan, M.M.S., and Sharp, H.T., 1991, "Massively parallel three-dimensional Euler/Navier-Stokes method," AIAA Journal, Vol. 29, No. 5, pp. 657-666. doi: 10.2514/3.10635

Papa, J.C., Azevedo, J.L.F., 2003, "Three dimensional flow simulations over a typical sounding rocket", Proceedings of the 21st AIAA Applied Aerodynamics Conference, AIAA Paper No. 2003-3421, Orlando, FL, USA.

Pio, D.M., Basso, E., Souza, C.E., Azevedo, J.L.F., and Silva, R.G.A., 2010, "Numerical simulations of the aerodynamic load distributions over the VS-30 sounding rocket," Proceedings of the 13th Brazilian Congress of Thermal Sciences and Engineering - ENCIT 2010, Uberlândia, MG, Brazil.

Pulliam, T.H., Steger, J.L., 1980, "Implicit finite-difference simulations of three-dimensional compressible flow," AIAA Journal, Vol. 18, No. 2, pp. 159-167. doi: 10.2514/3.50745

Strauss, D., Azevedo, J.L.F., 1999, "A numerical study of turbulent afterbody flows including a propulsive jet," Proceedings of the 17th AIAA Applied Aerodynamics Conference, AIAA Paper No. 99-3190-CP, Norfolk, VA, USA, pp. 654-664.

Turkel, E., Vatsa, V.N., 1994, "Effect of artificial viscosity on three-dimensional flow solutions," AIAA Journal, Vol. 32, No. 1, pp. 39-45.

Vieira, R., Azevedo, J.L.F., Fico Jr., N.G.C.R., and Basso, E., 1998, "Three dimensional flow simulation in the test section of a slotted transonic wind tunnel," Proceedings of the 21st Congress of the International Council of the Aeronautical Sciences, ICAS, Paper No. 98-R.3.11, Melbourne, Australia.

Wang, Z.J., Buning, P., and Benek, J., 1995, "Critical evaluation of conservative and non-conservative interface treatment for Chimera grids," Proceedings of the 33rd AIAA Aerospace Sciences Meeting and Exhibit, AIAA Paper No. 95-0077, Reno, NV, USA.

Wang, Z.F., Yang, H.Q., 1994, "A unified conservative zonal interface treatment for arbitrarily patched and overlapped grids," Proceedings of the 32nd AIAA Aerospace Sciences Meeting and Exhibit, AIAA Paper No. 94-0320, Reno, NV, USA.